Contents

Subject Index V
List of Locations VIII
Abraham, K., s. Ryabchikov, I.D., et al. 80
Allen, A.R., Stubbs, D.: An $^{40}AR/^{39}AR$ Study of a Polymetamorphic Complex in the Arunta Block, Central Australia 319
Armbrustmacher, T.J., Hedge, C.E.: Genetic Implications of Minor-Element and Sr-Isotope Geochemistry of Alkaline Rock Complexes in the Wet Mountains Area, Fremont and Custer Counties, Colorado 424
Basu, A.R., s. Domenick, M.A. 290
Bell, J.D., s. Harris, C. 107
Bevan, J.C.: Reaction Rims of Orthopyroxene and Plagioclase Around Chrome Spinels in Olivine from Skye and Rhum (NW Scotland) 124
Bodinier, J.L., s. Leyreloup, A., et al. 68
Bossière, G., s. Marchand, J., et al. 439
Brothers, R.N., Yokoyama, K.: Comparison of the High-Pressure Schist Belts of New Caledonia and Sanbagawa, Japan . . . 219
Byerly, G., s. Muehlenbachs, K. 76
Cann, J.R., s. Prichard, H.M. 46
Carmichael, D.M., s. Pattison, D.R.M., et al. 394
Chatterjee, N.D., s. Halbach, H. 337
Clemens, J.D, McMillan, P.F.: A Discussion of: "Biotite Melting in High-Grade Metamorphic Gneisses from the Haut-Allier (French Massif Central)" by Nédélec and Paquet (Discussion) 436
Clifford, P., s. Cox, K.G. 268
Cox, K.G., Clifford, P.: Correlation Coefficient Patterns and Their Interpretation in Three Basaltic Suites 268
Cygan, R.T., Lasaga, A.C.: Crystal Growth and the Formation of Chemical Zoning in Garnets 187
Dautria, J.-M., s. Leblanc, M., et al. 347
DeLong, S.E., s. Walker, D. 231
Dickin, A.P., s. Thompson, R.N., et al. 159
Dietvorst, E.J.L.: Retrograde Garnet Zoning at Low Water Pressure in Metapelitic Rocks from Kemiö, SW Finland . . . 37
Domenick, M.A., Basu, A.R.: Age and Origin of the Cortlandt Complex, New York: Implications from Sm-Nd Data 290
Dostal, J., s. Leyreloup, A., et al. 68
Dupuy, C., s. Leyreloup, A., et al. 68
Fiesinger, D.W., s. Nicholls, J., et al. 201
Fonarev, V.I., Graphchikov, A.A.: Experimental Study of Fe-Mg- and Ca-Distribution Between Coexisting Ortho- and Clinopyroxenes at $P = 294$ MPa, $T = 750$ and 800° C 311
Freer, R.: Diffusion in Silicate Minerals and Glasses: A Data Digest and Guide to the Literature (Correction) 106
Friedman, I., s. Lee, D.E., et al. 150
Furnes, H., Thon, A., Nordås, J., Garmann, L.B.: Geochemistry of Caledonian Metabasalts from Some Norwegian Ophiolite Fragments 295
Garmann, L.B., s. Furnes, A., et al. 295
Gibson, I.L., s. Thompson, R.N., et al. 159
Girod, M., s. Leblanc, M., et al. 347
Gleason, J.D., s. Lee, D.E. et al. 150
Gohn, E., s. Haack, U., et al. 279
Graphchikov, A.A., s. Fonarev, V.I. 311
Green, N.L.: Fluorine Geochemistry of Quaternary Volcanic Rocks from Southwestern British Columbia: Some Petrogenetic Implications 405
Green, T.H., Watson, E.B.: Crystallization of Apatite in Natural Magmas Under High Pressure, Hydrous Conditions, with Particular Reference to "Orogenic" Rock Series 96
Gupta, L.N., s. Johannes, W. 114
Haack, U., Hoefs, J., Gohn, E.: Constraints on the Origin of Damaran Granites by Rb/Sr and $\delta^{18}0$ Data 279
Halbach, H., Chatterjee, N.D.: An Empirical Redlich-Kwong-Type Equation of State for Water to 1,000° C and 200 Kbar 337
Hansen, E.C., s. Janardhan, A.S. 130
Harris, C., Bell, J.D.: Natural Partial Melting of Syenite Blocks from Ascension Island 107
Hedge, C.E., s. Armbrustmacher, T.J. 424
Hoefs, J., Müller, G., Schuster, A.K.: Polymetamorphic Relations in Iron Ores from the Iron Quadrangle, Brazil: The Correlation of Oxygen Isotope Variations with Deformation History . . . 241
Hoefs, J., s. Haack, U., et al. 279
Holm, P.E.: Non-Recognition of Continental Tholeiites Using the Ti-Y-Zr Diagram 308
Janardhan, A.S., Newton, R.C., Hansen, E.C.: The Transformation of Amphibolite Facies Gneiss to Charnockite in Southern Karnataka and Northern Tamil Nadu, India 130
Johannes, W., Gupta, L.N.: Origin and Evolution of a Migmatite 114
Kirkpatrick, R.J., s. Kuo, L.C. 13
Kisch, H.J., s. Padan, A., et al. 85
Koons, P.O.: An Experimental Investigation of the Behavior of Amphibole in the System Na_2O-MgO-Al_2O_3-SiO_2-H_2O at High Pressures 258
Kuo, L.-C., Kirkpatrick, R.J.: Pre-Eruption History of Phyric Basalts from DSDP Legs 45 and 46: Evidence from Morphology and Zoning Patterns in Plagioclase 13
Lancelot, J., s. Pin, C. 1
Lasaga, A.C., s. Cygan, R.T. 187
Leblanc, M., Dautria, J.-M., Girod, M.: Magnesian Ilmenite Xenoliths in a Basanite from Tahalra, Ahaggar (Southern Algeria) 347
Lee, D.E., Friedman, I., Gleason, J.D.: The Oxygen Isotope Composition of Granitoid and Sedimentary Rocks of the Southern Snake Range, Nevada 150
Leyreloup, A., Bodinier, J.L., Dupuy, C., Dostal, J.: Petrology and Geochemistry of Granulite Xenoliths from Central Hoggar (Algeria) – Implications for the Lower Crust 68
Leyreloup, A., s. Marchand, J., et al. 439
Marchand, J., Bossière, G., Leyreloup, A.: Pinite and Pseudo-"Glass" in High-Grade Metamorphic Gneisses. A Discussion of: "Biotite Melting in High-Grade Metamorphic Gneisses from the Haut-Allier (French Massif Central)" (Discussion) . . 439
McMillan, P.F., s. Clemens, J.D. 436
Milne, K.P., Starmer, I.C.: Extreme Differentiation in the Proterozoic Gjerstad-Morkeheia Complex of South Norway . . 381
Morrison, M.A., s. Thompson, R.N., et al. 159
Muehlenbachs, K., Byerly, G.: ^{18}O-Enrichment of Silicic Magmas Caused by Crystal Fractionation at the Galapagos Spreading Center 76
Müller, G., s. Hoefs, J., et al. 241
Naef, U., Stern, W.B.: Some Critical Remarks on the Analysis of Phengite and Paragonite Components in Muscovite by X-Ray Diffractometry 355
Nédélec, A., Paquet, J.: A Reply to Clemens and McMillan's, and Marchand, Bossière and Leyreloup's Discussions (Discussion) 443
Newton, R.C., s. Janardhan, A.S., et al. 130
Nicholls, J., Stout, M.Z., Fiesinger, D.W.: Petrologic Variations in Quaternary Volcanic Rocks, British Columbia, and the Nature of the Underlying Upper Mantle 201
Nordås, J., s. Furnes, A., et al. 295
Okay, A.I.: Incipient Blueschist Metamorphism and Metasomatism in the Tavşanlı Region, Northwest Turkey 361
Orville, P.M., s. Walther, J.V. 252
Padan, A., Kisch, H.J., Shagam, R.: Use of the Lattice Parameter b_o of Dioctahedral Illite/Muscovite for the Characterization of P/T Gradients of Incipient Metamorphism 85

Paquet, J., s. Nédélec, A. 443
Pattison, D.R.M., Carmichael, D.M., St-Onge, M.R.: Geothermometry and Geobarometry Applied to Early Proterozoic "S-Type" Granitoid Plutons, Wopmay Orogen, Northwest Territories, Canada 394
Pin, C., Lancelot, J.: U-Pb Dating of an Early Paleozoic Bimodal Magmatism in the French Massif Central and of Its Further Metamorphic Evolution 1
Prichard, H.M., Cann, J.R.: Petrology and Mineralogy of Dredged Gabbro from Gettysburg Bank, Eastern Atlantic 46
Reinecke, T.: Cymrite and Celsian in Manganese-Rich Metamorphic Rocks from Andros Island/Greece 333
Ryabchikov, I.D., Schreyer, W., Abraham, K.: Compositions of Aqueous Fluids in Equilibrium with Pyroxenes and Olivines at Mantle Pressures and Temperatures 80
Sack, R.O.: Spinels as Petrogenetic Indicators: Activity-Composition Relations at Low Pressures 169
Salje, E., Werneke, Chr.: The Phase Equilibrium Between Sillimanite and Andalusite as Determined from Lattice Vibrations 56
Schreyer, W., s. Ryabchikov, I.D., et al. 80
Schuster, A.K., s. Hoefs, J., et al. 241
Sekine, T., Wyllie, P.J.: Phase Relationships in the System $KAlSiO_4$–Mg_2SiO_4–SiO_2–H_2O as a Model for Hybridization Between Hydrous Siliceous Melts Peridotite 368
Sekine, T., s. Wyllie, P.J. 375
Selverstone, J.: Fluid Inclusions as Petrogenetic Indicators in Granulite Xenoliths, Pali-Aike Volcanic Field, Chile 28
Shagam, R., s. Padan, A., et al. 85
Starmer, I.C., s. Milne, K.P. 381
Stern, W.B., s. Naef, U. 355
St-Onge, M.R., s. Pattison, D.R.M., et al. 394
Stout, M.Z., s. Nicholls, J., et al. 201
Stubbs, D., s. Allen, A.R. 319
Thompson, R.N., Dickin, A.P., Gibson, I.L., Morrison, M.A.: Elemental Fingerprints of Isotopic Contamination of Hebridean Palaeocene Mantle-Derived Magmas by Archaean Sial . . . 159
Thon, A., s. Furnes, A., et al. 295
Vogel, T.A.: Magma Mixing in the Acidic-Basic Complex of Ardnamurchan: Implications on the Evolution of Shallow Magma Chambers 411
Walker, D., DeLong, S.E.: Soret Separation of Mid-Ocean Ridge Basalt Magma 231
Walther, J.V., Orville, P.M.: Volatile Production and Transport in Regional Metamorphism 252
Watson, E.B., s. Green, T.H. 96
Werneke, Chr., s. Salje, E. 56
Wyllie, P.J., Sekine, T.: The Formation of Mantle Phlogopite in Subduction Zone Hybridization 375
Wyllie, P.J., s. Sekine, T. 368
Yokoyama, K., s. Brothers, R.N. 219
Announcement: 27th International Geological Congress in Moscow, USSR 106
IMA News: 13th General Meeting in Varna, Bulgaria 446

Indexed in Current Contents/
Abstracted in Mineralogical Abstracts

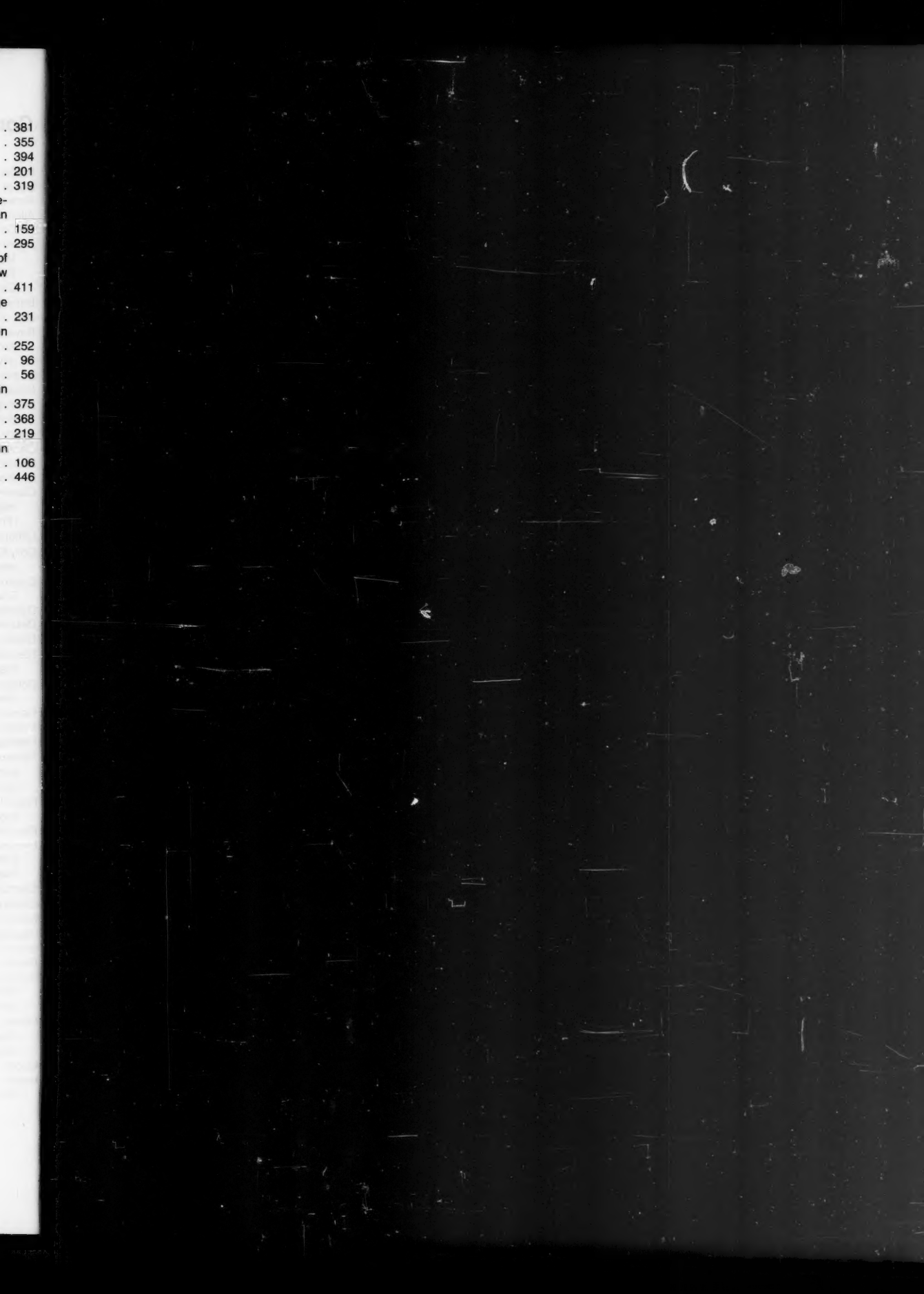

Sub

Actino
activity
adcum
aegirin
Al, sol
alaskit
albite
–, blue
Alice S
alkali f
alkali g
alkalin
alkali c
Al-silic
Al-spi
amorp
436
amphi
–, oce
–, –, C
amphi
amphi
–, volc
amphi
–, tran
anatex
andalu
andes
ankara
anorth
apatite
–, gne
–, high
arago
Ar iso
Arunta
augen
augite
–, top
in b

Ba-m
bande
basal
basal
basal
–, gra
–, pre
–, Ti-
basan
–, xen
batho
batho
394
–, –, t
biotite
425
–, me
biotite
dyn
biotite
blues
braun
burial

Subject Index

Actinolite 47, 219f.
activity – composition relations, spinels 169f.
adcumulates, Wet Mts. 425f.
aegirine – augite 427
Al, solubility in silicate melts 397
alaskite 134
albite 145, 225, 243, 261, 335, 427
–, blueschists 363f.
Alice Springs orogeny, Central Australia 326
alkali feldspar 320
alkali gabbro 426
alkaline igneous complexes, Colorado 424f.
alkali olivine basalt 201
Al-silicate triple point 65f., 401
Al-spinel, kimberlites 350f.
amorphous phase, electron beam experiments 436, 443
amphibole 425, 428
–, oceanic crust gabbro 47f.
–, –, Cl content 50
amphibole gabbro 290
amphiboles, experim. investigation 258f.
–, volcanics 405
amphibolite 242, 381f.
–, transition to charnockite 132f.
anatexis, gneiss 436f., 439f.
andalusite – sillimanite phase equilibrium 56f.
andesites, F-content 405f.
ankaramites 201
anorthosite 425
apatite 143, 397, 406, 425
–, gneiss and metagabbros 383f.
–, high-pressure crystallization in magmas 96f.
aragonite, veins in blueschists 365
Ar isotope dating method 319
Arunta orogeny, Central Australia 324f.
augen gneiss, S-Norway 381f.
augite 206, 405
–, topotactic replacement by Na-pyroxenes in blueschists 363f.

Ba-muscovite 335
banded iron ores, Precambrian 241f.
basaltic andesite, F-contents 405f.
basaltic suites, fractionation 268f.
basalts, Ardnamurchan 412f.
–, granulite xenoliths 28f.
–, pre-eruption history 13f.
–, Ti-Y-Zr data 308f.
basanite 201
–, xenoliths 347f.
batholith garnets 397f.
batholiths, Wopmay, geothermobarometry 394f.
–, –, tectonic implication 403
biotite 52, 115, 132f., 243, 320, 397f., 406, 425, 428
–, metagabbros 383f.
biotite-garnet geothermometer, thermodynamics 398
biotite melting, gneisses 436f., 445
blueschists 361f.
braunite 333
burial metamorphism 219f.

Calcite 334
carbonatites 425
cation ordering, spinels 178f.
celsian 333f.
charnockites 130f., 318, 384
chemical analysis
–, albite, blueschists 364
–, amphiboles, metagabbros 385
–, Ardnamurchan complex 413f.
–, –, oceanic crust gabbros 50
–, augen gneiss, S-Norway 387
–, biotites, anatectic gneisses 441
–, –, charnockites 142
–, –, Wopmay batholiths 396
–, blueschist minerals, Turkey 364
–, celsian, Andros 335
–, charnockites, India 137f.
–, chlorite, blueschists 364
–, –, oceanic crust gabbros 53
–, clinopyroxenes, charnockites 139
–, –, metagabbros 385
–, comendite, Ascension 109
–, cummingtonites, metagabbros 385
–, cymrite, Andros 335
–, gabbro, Ardnamurchan 413
–, garnet, blueschists 364
–, –, charnockites 141
–, –, metapelites 39
–, –, Wopmay batholiths 396
–, glass, Ascension syenite 110
–, granite, Ascension 109
–, granodioritic gneisses, S-Norway 387
–, granulitic xenoliths, Hoggar basalts 70
–, greenstones, Norwegian ophiolites 299
–, hornblendes, charnockites 140
–, ilmenite, garnet inclusions 39
–, lavas, Brit. Columbia 205
–, lawsonite, blueschists 364
–, metadiorites, S-Norway 386
–, metagabbros, S-Norway 386
–, Mg-ilmenites, Ahaggar kimberlites 349
–, olivine, lavas, Brit. Columbia 206
–, –, S-Norwegian metamorphic rocks 385
–, ophiolites, Norway 297f.
–, orthopyroxenes, charnockites 139
–, –, metagabbros 385
–, pelites, average 253
–, pinites, anatectic gneisses 441
–, plagioclase, lavas, Brit. Columbia 210
–, –, mid-ocean ridge basalts 17
–, –, Wopmay batholiths 396
–, pumpellyite, blueschists 364
–, pyroxenes, lavas, Brit. Columbia 208
–, –, oceanic crust gabbros 52
–, sodic pyroxenes, blueschists 364
–, Ti-magnetites, Ahaggar kimberlites 351
chemical zoning, garnets 187f.
chert 295
chlorite 142, 225, 243, 440
–, blueschists 364f.
–, oceanic crust gabbros 47, 52
chloritoid 243
chromite 169f.
cinder cones 201f.
Cl, oceanic crust amphiboles 51
clinochlore 53
clinopyroxene 28f., 47, 69, 139, 235, 290, 305, 425
–, coex. with orthopyroxenes, experim. element distribution 311f.
–, metagabbros 383f.
clinopyroxenite 290
clinozoisite 243
comendite 109
conglomerate 242
contamination, Hebridean lavas 160f.
cordierite 243, 320, 397
–, alteration 436f., 439f.
coronite metagabbro 3
correlation coefficient pattern, fractionation of basaltic suites 270f.
cortlandite 290
Cr-spinel, reaction rims 124f.
crystal fractionation, mid-ocean ridge basalts 231f.
crystallinity index, illites 86f.
crystal mush, garnet xenocrysts 397f.
cummingtonite, metagabbros 383f.
cumulus minerals, Mc Clure Mt. Complex 425
cumulus orthopyroxene, mid-ocean ridge gabbro 236
cymrite, occurrence 333
–, parageneses 334

Dacites, F-contents 405f.
deformation, Brazilian iron ores 244f.
–, relation to garnet growth 43
deformation textures, oceanic crust gabbro 47f.
devolatilization reactions, metamorphism 253f.
diamonds, ilmenite inclusions 347f.
differentiation, granitoids 150f.
–, S-Norway meta-igneous rocks 381f.
diffusion in silicates, corrected data 106
diopside 134, 243
diorite 290
dolerites 275, 363
dolomite 242
dyke complexes, Norway 297

Eclogites 352
edenite 325
elemental correlation, basaltic suites 268f.
enderbite 69
enstatite, melting reactions 369f.
epidote 145
exsolutions, Ti-magnetite in Mg-ilmenite, kimberlites 349

F, analytical procedure in volcanic rocks 406
–, influence on biotite stability 401
–, relation to phenocrysts, volcanics 407
–, volcanic rocks 405f.
fassaite 350
fayalite mangerite, S-Norway 381
feldspars, S-Norwegian metamorphic rocks 387f.

fluid inclusions, granulite xenoliths 28f.
fluid transport, metamorphism 256
fluorite 428
fractional crystallization 416
–, behaviour of F 408
–, Norwegian metabasalts 303
fractionation, basaltic suites 268f.
–, Soret effect in silicate melts 231f.
fractionation models, garnet zoning 187f.

Gabbro 46f., 236, 295, 428
garnet 69, 135, 397
–, blueschists 365
–, crystal growth and chemical zoning 187f.
–, exchange equilibrium fractionation model 188f.
–, isothermal fractionation model 187f.
–, origin in granitoid plutons 397f.
–, retrograde zoning 37f.
garnet-biotite-thermometer, geothermobarometry 395f.
geikielite 352
geochronology, metamorphic terrains 319f.
geothermobarometry, charnockites 144
–, Wentzel and Hepburn plutons 394f.
geothermometry, lavas, British Columbia 211
–, two-pyroxenes –, Norwegian metagabbro 386
glass, biotite melting 436f., 441f.
–, granulitic xenoliths 69
–, syenites 109
glaucophane 225, 258
glaucophane-lawsonite zone, blueschists 362f.
glomerocrysts, basalts 13f.
gneiss 4, 320
–, anatexis 436f., 439f.
–, S-Norway 381f.
–, transformation to charnockite 130f.
granite 109, 132f., 324, 395f.
–, O isotopic data 150f.
–, Rb-Sr data 280f.
granitic charnockites 131f.
granulites 130f., 318
–, xenoliths 68f.
–, –, fluid inclusions 28f.
granulitic charnockites 131f.
greenschists, blueschist zone 362
greenstones, Norway 295f.
grossular – sillimanite – quartz – anorthite barometer 395f.

Hawaiites 201
hematite, kimberlite xenoliths 350
hematite ores, Brazil 241f.
high-pressure belts 219f.
H_2O hybridization reactions 372f.
hollandite 335
hornblende 132f., 320
–, retention of Ar, chemical control 328
hornblende andesites, F-contents 405f.
hornblende-biotite syenite 426f.
hornblendite 290
hybridization, siliceous melts 368f.
hypersthene 201
hypersthene andesites, F-contents 405f.
hypersthene gabbro 412

Ijolite 425
illite crystallinity 85f.
ilmenite 143, 406
–, kimberlites 347f.
–, metagabbros 383f.
ilmenitite xenoliths 347f.
immiscibility, siliceous melts 416
intercumulus minerals, syenites 427
intermediate igneous rocks, origin by magma mixing 416f.
inverse zoning, garnets 41
isothermal hybridization, siliceous melts – peridotite reaction 371f.
isotopic contamination, Hebridean lavas 159f.
itabirites 241f.

Jacupirangite 426
jadeite 261
jasper 295
juvite 426

Kaersutite 350
kaolinite, cordierite alteration 436f.
K-feldspar 69, 115, 134f., 397
kimberlites 347f.
kimberlitic spinels 347f.
kink bands, Ti-magnetite in kimberlites 348
kulkeite 259f.
kyanite 243, 440

Lava 108
–, Garibaldi Lake 405f.
–, isotopic contamination 159f.
–, Snake River plain 201f.
lava flows 201f.
lawsonite 224
–, blueschist zone 362f.
layered gabbro 297
leptynite 3f.
leucosome 115
lherzolite 204f.
lutite 295

Magma chambers 411
magma genesis, subducted crust 378
magma mixing 411f.
–, basalts 24
magnetite 143, 211, 242f., 405, 425
malignite 426
mangerite 385f.
mantle diapirism 352
marble 242
–, blueschist contacts 362f.
martite 242
megacrysts, basalts 14f.
melange, blueschist zone 362
melanosome 114
melteigite 426
melting reactions, system $KAlSiO_4$-Mg_2SiO_4-SiO_2-H_2O 369
melt-peridotite reactions 368f.
mesosome 114
meta-anorthosite 69
metabasalts, Norwegian ophiolites, rare earth element patterns 300
–, ophiolite fragments 295f.
metadiorites, S-Norway 383f.
metagabbros, S-Norway 383f.
meta-hyaloclastites 297
metamorphic terrains, Arvika migmatites 11
–, dating 319f.
metamorphism, Andros 333f.
–, Arunta gneiss 320f.
–, blueschists 361f.
–, b_0 of micas as P/T indicator 85f.
–, high-pressure belts 219f.
–, Massif Central 1f.
–, volatile production 252f.
metasomatism, blueschists 361f.
–, charnockite formation 132f.
–, Precambrian iron ores 241f.
–, subducted crust 377
Mg-ilmenites, kimberlites 347f.
Mg-riebeckite 243
micas, b_0 as P/T indicator 85f.
microcline 118
microperthite 426
mid-ocean ridge basalts, ^{18}O enrichment 7
–, Soret separation 231f.
migmatites 131f.
–, development 114f.
Minas metamorphism 242
Mn-pyroxenes 335
Mn-tremolite 335
Moho, depth in Brit. Columbia 203
montmorillonite 52
muscovite 243, 334, 397, 427, 440
–, b_0 as P/T indicator 85f.
–, lattice parameters 355f.
mylonites 320

Nepheline 427f.
nepheline syenite 426f.
nephelinites 201
net-veining 412f.
nodules, Mg-ilmenites in kimberlites 347f.
norite 290

Oceanic crust, subduction 376f.
^{18}O enrichment, crystal fractionation in magm 76f.
O isotopic data, Damara granites 280f.
–, granitoids 150f.
–, itabirites 243f.
oligoclase 132
olivine 13f., 29, 47, 124, 205, 235, 305, 34 405, 425, 427
olivine-spinel Fe-Mg exchange equilibria 175f.
olivine tholeiite 201
omphacite 224
ophiolites 295f., 362
orthoamphibole 145
ortholeptynite 3
orthopyroxene 28f., 69, 134f., 236, 405
–, coex. with clinopyroxenes, experim. eleme distribution 311f.
–, metagabbros 383f.
–, reaction rim around Cr-spinel 127f.

Paleosome 114
paragneiss 115
paragonite 225, 261
–, determination in muscovite 355f.

partial melting, gneiss 436
–, subducted crust 378
–, syenite 107f.
pegmatite 6f.
pelite, metamorphic volatile production 252f.
penninite 53
peridotite 124, 361
–, reaction with siliceous melts 368f.
peridotite-melt reactions 375f.
perthite, metagabbro 383f.
phase relationships, siliceous melt – peridotite reactions 368f.
phengite component, determination in muscovite 355f.
phenocrysts, volcanics, F-contents 406f.
phlogopite 320
–, melting reactions 369f.
–, subduction zone hybridization 375f.
phonon spectra, Al-silicates 58f.
phyric basalts, mid-ocean ridge 13f.
picrite, mid-ocean rift valley 235
piemontite 335
pillow breccias 297
pillow lavas 295
pillows, intermediate volcanic rocks 412f.
pinite 436, 439f., 443f.
plagioclase 13f., 29, 69, 114f., 124, 132, 209, 235, 243, 276, 305, 320, 397, 405, 412, 425f.
–, metagabbros 383f.
–, oceanic crust gabbro 47, 51
–, reaction rim around Cr-spinel 129
–, zoning 16f.
plagiogranite 295
plate tectonics 219f.
pleonast 69, 169f.
plutons, geothermobarometry 394f.
P_2O_5, intermediate igneous rocks 420
P_2O_5-SiO_2 systematics, orogenic rock series 100
preiswerkite 261f.
pseudo-brookite 350
pumpellyite 219f.
–, blueschists 365
P-V-T data, water 339f.
pycnochlorite 53
pyribolites, S-Norway 381f.
pyriclasite 69
pyrigarnites 5
pyrolite, partial melting 215
pyroxenes, coex., Fe-Mg-Ca distribution 311f.
pyroxenite 290, 425
pyroxenolite 69f.

Quartz 69, 108, 115, 145, 225, 242f., 261, 334
–, pinite 440
quartz gabbro 412
quartz iron formations 241f.
quartzite 133, 242, 333
quartz syenite 428

Raman microspectroscopy, glasses 444
rare earth elements, alkaline igneous rocks 428f.
–, net-veined complex 417
–, Norwegian ophiolites 298f.
Rb/Sr data, Damara granites 279f.
recrystallization episodes, Arunta gneiss 320f.
Redlich-Kwong type equation of state for water 337f.
retrograde zoning, garnets 37f.
ring dikes 412, 425f.
ripidolite 53
rutile 69

Sanbagawa belt, isograds 223
–, mineral assemblages 224
–, pressure-temperature path 224
–, tectonic framework 222
sapphirine 69
seawater-basalt interaction 301
separation, Soret effect in melts 233f.
serpentinite 295
–, blueschist zone 362f.
shield terranes, metamorphism 130f.
silicate liquids, experim. investigation of Soret effect 232f.
sillimanite 69, 243, 397f., 436, 440, 444
sillimanite-andalusite phase equilibrium 56f.
Sm-Nd data, Cortlandt complex 290f.
solubility studies, system Mg_2SiO_4-SiO_2-H_2O 80f.
Soret effect 231f.
specularite 243
sphene 427
spilites 363
spinel 28f., 69, 425
–, acitivity-composition relations 169f.
–, exsolution in Ti-magnetites 348f.
Sr isotope ratios, alkaline igneous rocks 431f.
staurolite 247
step-degassing technique, Ar isotopes dating 319f.
stilpnomelane 243
stromatic migmatite, development 114f.
S-type pluton 395f.
subducted crust, melting 373
subduction 219f.
subduction zone hybridization 368f., 375f.
syenite 425f.
–, natural partial melting 107f.
symplectite 29
systems, $KAlSi0_4$-Mg_2SiO_4-SiO_2-H_2O 368f.
–, Mg_2SiO_4-SiO_2-H_2O, high-pressure solubility experiments 80f.
–, Na_2O-MgO-Al_2O_3-SiO_2-H_2O, amphibole behaviour 258f.

Talc 53, 243, 261
thermal diffusion 231f.
thermodynamics, biotite-garnet-geothermometer 398
–, grossular-anorthite-sillimanite-quartz geobarometry 398
–, spinels 170f.
tholeiites, Ti-Y-Zr diagram 308f.
TiO_2, intermediate igneous rocks 420
titanomagnetite 347, 406
Ti-Y-Zr diagram, tholeiites 308f.
tonalite 295
trace elements, Ardnamurchan complex 418
–, Hebridean lavas 161f.
–, Norwegian ophiolites 298
trondhjemite 5
two-stage processes, basaltic fractionation 269f.

U-Pb dating, meta-igneous rocks 1f.
upper mantle, Brit. Columbia 214
–, magma equilibration 216
–, xenoliths, Mg-ilmenites 353
urtite 426

Volatile production, metamorphism of pelites 254
volcano-sedimentary sequence, blueschist metamorphism 361f.

Water, Redlich-Kwong type equation of state 337f.
wonesite 261
Wood and Banno geothermometer 317

Xenocrysts, garnets in batholiths 397f.
xenoliths, granulites in basalts 68f.
–, Mg-ilmenitites 347f.
–, Snake River volcanics 201f.

Zircon 397, 428
–, gneiss, age determination 6f.
zoisite 225, 263
zoning, garnets 39f., 187f.
–, plagioclases 21f.

List of Locations

Adrar N'Addjer Massif, Hoggar 68
Ahaggar, Algeria 68, 347
Aiyansh River region, Brit. Columbia 202
Alert Bay Volcanic Belt, Brit. Columbia 406
Alice Springs, Central Australia 320
Anahim Volcanic Belt, Brit. Columbia 406
Andros, Greece 333
Anechowkur, Karnataka 132
Ankala Block, Arunta 321
Ardnamurchan, Scotland 411
Arunta Block, Central Australia 320
Arvika, Sweden 115
Ascension Isl., Atlantic 107
Atakor Massif, Hoggar 68
Atlin Lake region, Brit. Columbia 202

Bergen, Norway 296
Bhavani Sagar, Tamil Nadu 132

Can Young Canyon, Nevada 150
Clinker Peak, Garibaldi Lake 406
Cortlandt, New York 291
Custer Co., Colorado 425

Damara, Namibia 280
Democrat Creek Complex, Colorado 425
Dinbhum, Tamil Nadu 132
Doddabetta, Tamil Nadu 132

Fremont Co., Colorado 425

Galapagos Spreading Center, Pacific 76
Garibaldi Lake, Brit. Columbia 202, 406
Gem Park Complex, Colorado 425
Gettysburg Bank, Atlantic 46
Gjerstad-Morkeheia Complex, S-Norway 382
Gullfjellet, Norway 296

Harry Creek Area, Arunta 320
Haut-Allier, France 436, 439
Helvetic Nappe, Swiss Alps 88
Hepburn Pluton, Wopmay Orogen 395
Hoggar, Algeria 68, 347
Hullahalli, Karnataka 132

Iceland 270
Itabirito, Minas Gerais, Brazil 242
Itcha Mts. Complex, Brit. Columbia 202

Jämtland, Sweden 87
Juan de Fuca Plate 201

Kabbal, Karnataka 132
Karmøy, Norway 296
Karnataka, India 132
Kemiö, SW-Finland 37
Kious Basin, Nevada 150
Kütahya, Turkey 361

Lexington Creek, Nevada 150
Lykling, Norway 296

Mahabaleshwar, Deccan, India 270
Marvejols, Massif Central 3
Massif Central, France 3
Mc Clure Mt. Complex, Colorado 425
Menderes Massif, Turkey 361
Mid-Atlantic Ridge 25
Mt. Garibaldi region, Brit. Columbia 202, 406
Mt. Price, Garibaldi Lake 406
Mull, Hebrides, NW-Scotland 159

New Caledonia 220
Nilgiri Hills, Tamil Nadu 132

Okahandja, Damara 280
Okombahe, Damara 280
Omaruru, Damara 280
Osceola, Snake Range 150
Ouro Preto, Minas Gerais, Brazil 242

Pali-Aike, Chile 28
Pemberton Volcanic Belt, Brit. Columbia 4
Penninic Nappe, Swiss Alps 88
Pole Canyon, Nevada 150
Pueblos del Sur Area, Venezuela 88
Pykara, Tamil Nadu 132

Quadrilatero Ferrifero, Brazil 242

Rhum, Hebrides, NW-Scotland 124
Rooi Rand, Karoo, South Africa 270

Sanbagawa Belt, Japan 220
Shikoku, Japan 221
Skålvaer, Norway 296
Skye, Hebrides, NW-Scotland 124, 159
Snake Creek Area, Nevada 150
Snake Range, Nevada 150
Snake River Plain, Nevada 202
Solund, Norway 296
Stavfjorden, Norway 296
Stikine River Region, Brit. Columbia 202
Swarnavati, Karnataka 132

Tahalra, Ahaggar 347
Tamanrasset, Ahaggar 347
Tamil Nadu, India 132
Tavşanlı, Turkey 361
Temple Hill, Karnataka 132

Utralanama Block, Arunta 321

Vitali, Andros 333

Wentzel Pluton, Wopmay Orogen 395
Wet Mts., Colorado 425
Williams Canyon, Nevada 150
Wopmay Orogen, NW-Territories, Canada

Yelachipalaiyam, Karnataka 132
Young Canyon, Nevada 150

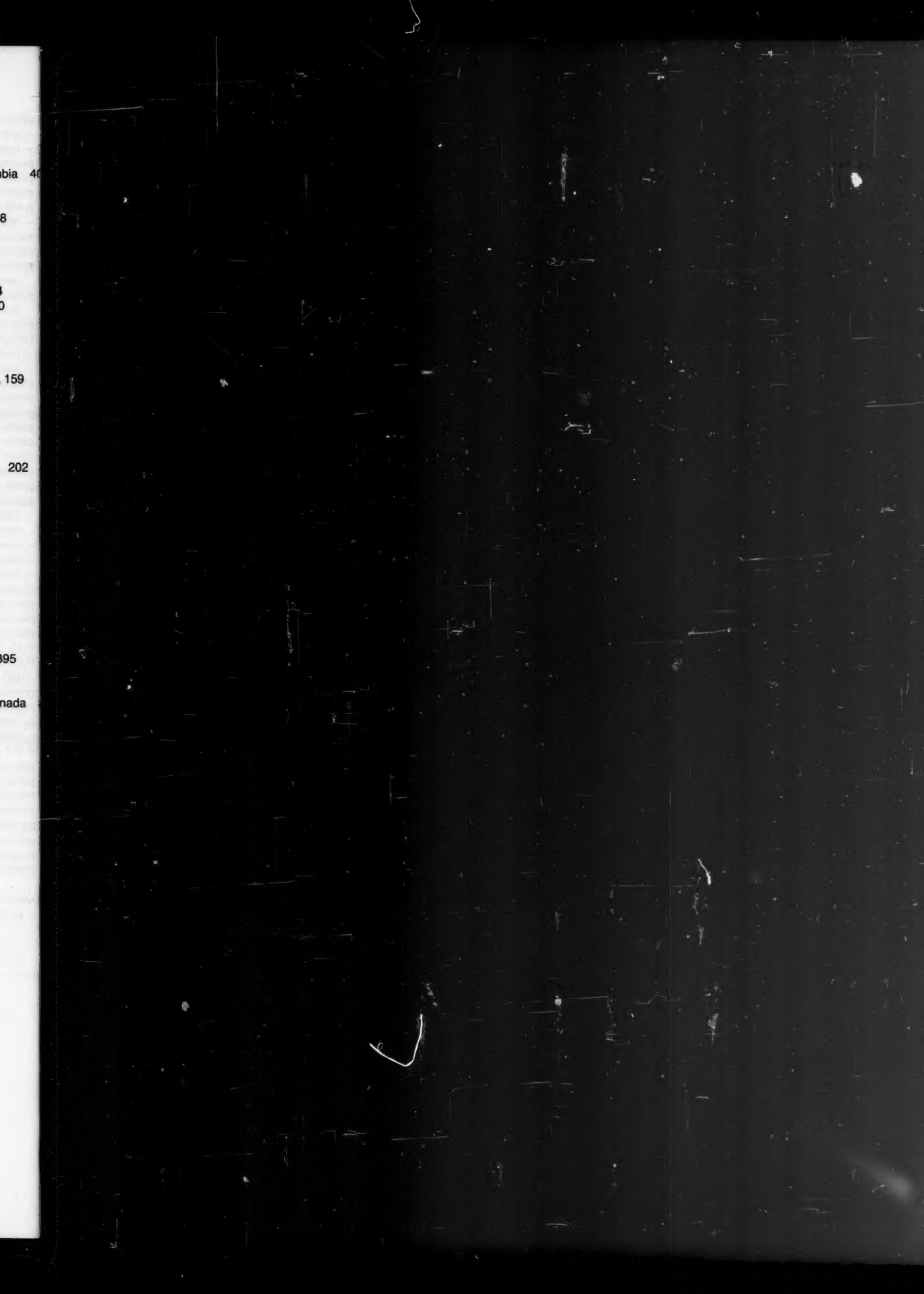

List of Locations

Adrar N'Addjer Massif, Hoggar 68
Ahaggar, Algeria 68, 347
Aiyansh River region, Brit. Columbia 202
Alert Bay Volcanic Belt, Brit. Columbia 406
Alice Springs, Central Australia 320
Anahim Volcanic Belt, Brit. Columbia 406
Andros, Greece 333
Anechowkur, Karnataka 132
Ankala Block, Arunta 321
Ardnamurchan, Scotland 411
Arunta Block, Central Australia 320
Arvika, Sweden 115
Ascension Isl., Atlantic 107
Atakor Massif, Hoggar 68
Atlin Lake region, Brit. Columbia 202

Bergen, Norway 296
Bhavani Sagar, Tamil Nadu 132

Can Young Canyon, Nevada 150
Clinker Peak, Garibaldi Lake 406
Cortlandt, New York 291
Custer Co., Colorado 425

Damara, Namibia 280
Democrat Creek Complex, Colorado 425
Dinbhum, Tamil Nadu 132
Doddabetta, Tamil Nadu 132

Fremont Co., Colorado 425

Galapagos Spreading Center, Pacific 76
Garibaldi Lake, Brit. Columbia 202, 406
Gem Park Complex, Colorado 425
Gettysburg Bank, Atlantic 46
Gjerstad-Morkeheia Complex, S-Norway 382
Gullfjellet, Norway 296

Harry Creek Area, Arunta 320
Haut-Allier, France 436, 439
Helvetic Nappe, Swiss Alps 88
Hepburn Pluton, Wopmay Orogen 395
Hoggar, Algeria 68, 347
Hullahalli, Karnataka 132

Iceland 270
Itabirito, Minas Gerais, Brazil 242
Itcha Mts. Complex, Brit. Columbia 202

Jämtland, Sweden 87
Juan de Fuca Plate 201

Kabbal, Karnataka 132
Karmøy, Norway 296
Karnataka, India 132
Kemiö, SW-Finland 37
Kious Basin, Nevada 150
Kütahya, Turkey 361

Lexington Creek, Nevada 150
Lykling, Norway 296

Mahabaleshwar, Deccan, India 270
Marvejols, Massif Central 3
Massif Central, France 3
Mc Clure Mt. Complex, Colorado 425
Menderes Massif, Turkey 361
Mid-Atlantic Ridge 25
Mt. Garibaldi region, Brit. Columbia 202, 406
Mt. Price, Garibaldi Lake 406
Mull, Hebrides, NW-Scotland 159

New Caledonia 220
Nilgiri Hills, Tamil Nadu 132

Okahandja, Damara 280
Okombahe, Damara 280
Omaruru, Damara 280
Osceola, Snake Range 150
Ouro Preto, Minas Gerais, Brazil 242

Pali-Aike, Chile 28
Pemberton Volcanic Belt, Brit. Columbia 40
Penninic Nappe, Swiss Alps 88
Pole Canyon, Nevada 150
Pueblos del Sur Area, Venezuela 88
Pykara, Tamil Nadu 132

Quadrilatero Ferrifero, Brazil 242

Rhum, Hebrides, NW-Scotland 124
Rooi Rand, Karoo, South Africa 270

Sanbagawa Belt, Japan 220
Shikoku, Japan 221
Skålvaer, Norway 296
Skye, Hebrides, NW-Scotland 124, 159
Snake Creek Area, Nevada 150
Snake Range, Nevada 150
Snake River Plain, Nevada 202
Solund, Norway 296
Stavfjorden, Norway 296
Stikine River Region, Brit. Columbia 202
Swarnavati, Karnataka 132

Tahalra, Ahaggar 347
Tamanrasset, Ahaggar 347
Tamil Nadu, India 132
Tavşanlı, Turkey 361
Temple Hill, Karnataka 132

Utralanama Block, Arunta 321

Vitali, Andros 333

Wentzel Pluton, Wopmay Orogen 395
Wet Mts., Colorado 425
Williams Canyon, Nevada 150
Wopmay Orogen, NW-Territories, Canada
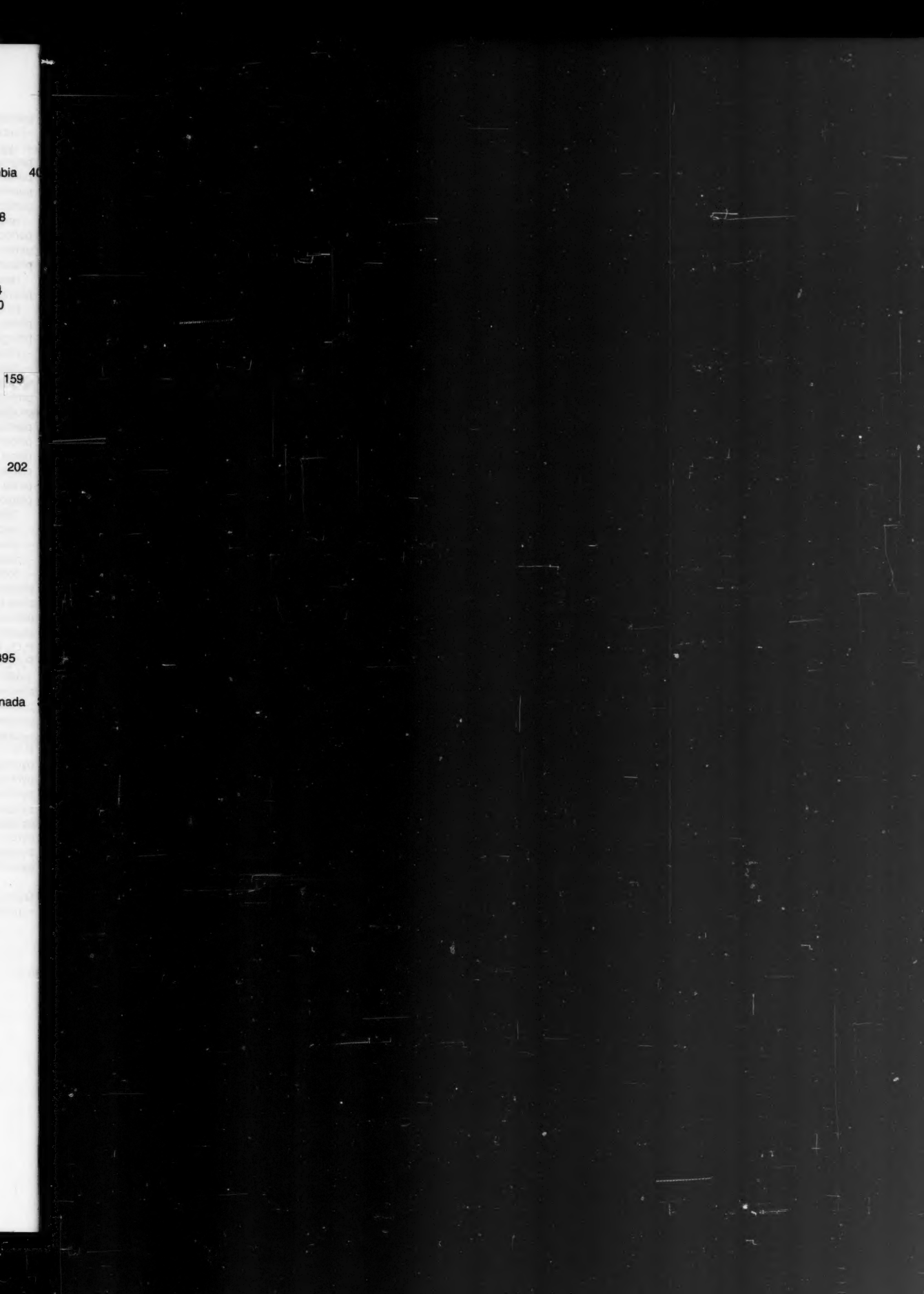
Yelachipalaiyam, Karnataka 132
Young Canyon, Nevada 150